

Antioxidant Activity of AuPt Nanoparticle with Square-Wave Pulse Deposition Method

Devi Indrawati Syafei*

National Taiwan University No.1, Section 5, Roosevelt Rd, Da'an District, Taipei City, Taiwan

*Corresponding author: r11527984@ntu.edu.tw

Received

31 May 2024

Received in revised form

24 June 2024

Accepted

28 June 2024

Published online

30 June 2024

DOI

<https://doi.org/10.56425/cma.v3i2.79>



Original content from this work may be used under the terms of the [Creative Commons Attribution 4.0 International License](https://creativecommons.org/licenses/by/4.0/).

Abstract

Gold nanoparticles and platinum nanoparticles are considered to be effective antioxidants due to their ability in inhibiting free radicals. In this research, AuPt nanoparticles were synthesized using a square wave pulse deposition method by varying the lower potential (E_L). The XRD results stated that AuPt nanoparticles had formed on the FTO substrate. The shape of AuPt nanoparticles is an irregular sphere in SEM-EDX characterization. EDX characterization also concluded that AuPt nanoparticles had formed on the FTO substrate. Antioxidant testing using the DPPH test resulted the largest inhibition value for AuPt NPs, with a lower potential of -0.6 V and the inhibition activity of 77.17%.

Keywords: antioxidant activity, electrodeposition, AuPt nanoparticles.

1. Introduction

The effectiveness of natural antioxidants and some synthetic antioxidants is limited because they are poorly absorbed, difficult to pass through cell membranes, and degraded during shipping, making them less effective. However, some nanoparticles from metal materials can be used as new antioxidants with superior characteristics [1–3].

Metal nanoparticles have received much attention and study in various aspects. Its properties, which can increase stability, increase yields, and reduce production costs are the reasons for conducting this nanoparticle study. The metal that is often used is gold (Au) [4–6]. Gold has low cytotoxicity and gold is known for its activity as an inhibitor of free radicals, which cause damage to various parts of cells that trigger aging [7]. From several reported studies, the kinetic behaviour of radical scavenging activity carried out in vivo or in vitro shows that gold-nanoparticles (AuNPs), which function as antioxidants, have a high kinetic effect in scavenging ROS (reactive oxygen species) in living cells [1,8]. When compared with natural antioxidants, synthetic antioxidants made from gold nanoparticles have three times more effective antioxidant activity [9] and do not have carcinogenic effects in the body [7,10].

Another nanoparticle is platinum nanoparticles (Pt NPs). Pt NPs have many uses, including as a catalyst [11–14] and as an antioxidant to reduce ROS in organisms [15].

Many studies have been carried out to examine that Pt NPs are also able to inhibit free radicals in the human body. In addition, Pt NPs has low cytotoxicity to cells and is not easily corroded. Therefore, this research will use the combination of gold-platinum nanoparticles (AuPt NPs) for the antioxidant activity.

There are many methods used for synthesizing nanoparticles, such as chemical reduction, Turkevich, Brust-Schiffrin, seeding growth, and green synthesis [4,16–19]. However, these methods use large amounts of energy, have high costs, use toxic solvents, and can be dangerous for the environment [20]. Besides that, the synthesis using the Turkevich, or biosynthesis method may lead to a discrepancy in antioxidant activity in the sample because other compounds are being used. In this research, gold nanoparticles will be synthesized using the electrodeposition method, which has many advantages, such as a fast process, low cost, being free from porosity, high purity, being capable of producing various shapes of nanoparticles, being capable of producing particle structures with sizes ranging in nanometre (nm), being easy to control the composition of the mixture, and no postdeposition treatment [21–24]. The electrodeposition method produces AuPt nanoparticles with a solid or film phase that does not use additives, so it does not affect antioxidant activity [25].

2. Materials and Method

The materials used in this research were HAuCl₄ (Merck), K₂PtCl₆ (Merck), Ethanol p.a. (Merck), ITO substrate, KCl (Merck), and DPPH (2,2-diphenyl-1-picrylhydrazyl). AuPt NPs were synthesized using the electrodeposition method (square wave pulse deposition). A 15-mL solution containing 0.8 mM K₂PtCl₆·6H₂O and 0.2 mM HAuCl₄·3H₂O and dissolved in 0.1 M KCl electrolyte were used in this synthesis. Synthesis was carried out at lower potential of -0.1 V, -0.6 V, and -1.0 V, with a synthesis time of 10 minutes. Pt wire was used as a counter electrode, and Ag/AgCl (KCl 3 M) as a reference electrode. Synthesis was carried out at room temperature (25°C).

AuPt NPs were characterized by energy dispersive X-ray spectroscopy (EDX, Oxford Instrument: Xplor 15) to obtain information regarding the composition of Au and Pt. Scanning Electron Microscope (SEM, ThermoScientific: Quanta 650) to carry out sample morphology analysis. X-ray diffraction (XRD Panalytical aeries) characterization to characterize the AuPt phase formed.

The DPPH test was carried out to determine the antioxidant activity of AuPt NPs using a microplate reader spectrophotometer (Thermo Scientific: Elisa Reader). The AuPt thin film was positioned on a microplate reader and incubated. The specimen was shaken and measured every 15 minutes until it reached 210 minutes. Inhibition of DPPH is then measured by the formula (equation 1):

$$\%DPPH \text{ inhibition} = \frac{[DPPH]}{[Control]-[DPPH]} \times 100\% \quad (1)$$

The inhibition calculation is then calculated at the absorbance peak, which is located at a wavelength of 516 nm.

3. Results and Discussion

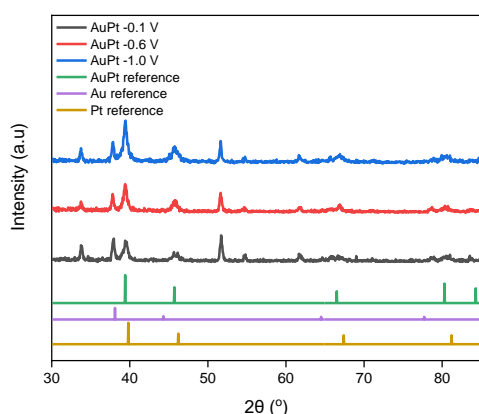


Figure 1. XRD diffraction of AuPt NPs.

XRD characterization was carried out to determine the formation of the AuPt phase in samples synthesized using the square wave pulse deposition method. Figure 1

represents the diffraction patterns of AuPt NPs, Pt NPs, and Au NPs. The XRD diffraction pattern of Au NPs is located at peaks 38.2°, 44.36°, 64.5°, and 77.52° [26]. Peaks for Pt NPs are at 39.7°, 46.2°, 67.4°, and 81.3° (Xiao, 2004). Reference AuPt samples are at 39.4°, 45.7°, 66.5°, and 80.3° [27]. Finally, AuPt samples synthesized at lower potential variations are located at 39.5°, 45.7°, 51.7°, 61.7°, 66.7°, and 80.5°. These results indicate that AuPt has been successfully formed in substrate. Additionally, peak at 38.4° was formed in the diffraction pattern. This peak is indicated by the AuNPs phase and is present in all lower potential applied samples [28]. Another peak at 51.7° comes from the substrate used for sample synthesis.

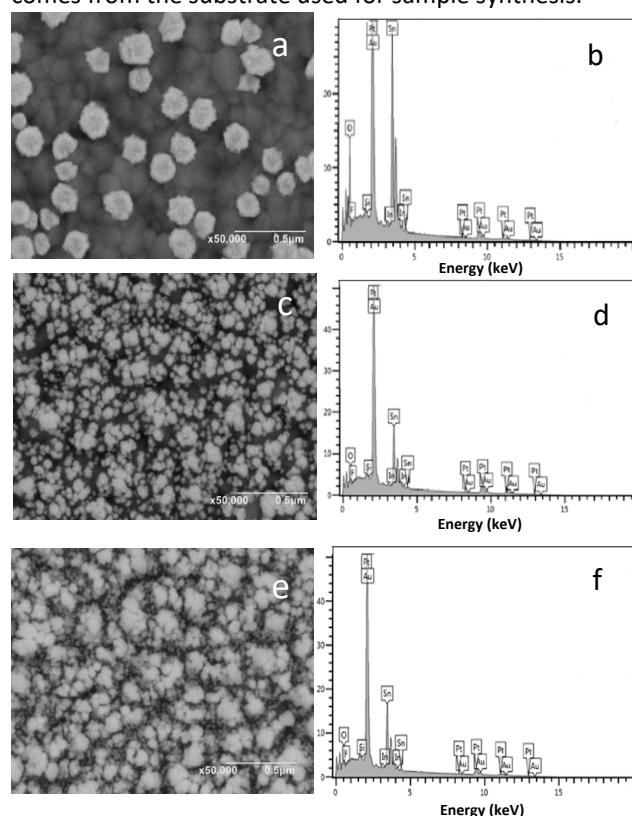


Figure 2. FESEM and EDX point analysis on AuPt NPs with lower potential application (a,b) -0.1 V; (c,d) -0.6 V; and (e,f) -1.0 V.

Figure 2 shows the morphology of AuPt with a spherical and irregular shape that is evenly distributed. The smaller the potential applied, the more Au and Pt are deposited. In addition, the size of AuPt also becomes smaller as the negative potential is applied. Nucleation of Pt and Au ions occurs at a certain potential, where Pt can nucleate at a potential of -0.1 V to -0.2 V and Au nucleates well at a potential of -0.4 V. If a more positive potential is applied, it will cause a slowdown in nucleation. Therefore, AuPt at EL -0.1 V has a relatively small number of particles because the applied potential is not very effective for Au and Pt nucleation. In addition, the visible SEM morphology of AuPt is less, proving that the nucleation of Pt and Au is not very effective at this potential. This is in accordance with research from Chiang et al [29], which states that gold can

be deposited well in the lower potential range below -0.4 V for gold nanoparticle nucleation and growth. Furthermore, the growth of Au and Pt particles occurred up to a potential of 1.0 V.

EDX point analysis was carried out to confirm the formation of Au and Pt elements. The results of the EDX analysis are shown in Figure 2. The Pt element signal was confirmed at 2.0–2.5 keV, and Au was confirmed at 2.0–2.1 keV in all EDX spectrum in figure 2b, 2d, and 2f. This is in accordance with research from Naderi et al [30], which stated that the Au signal on EDX was detected at 2.1 keV and Pt at 2.0–2.5 keV.

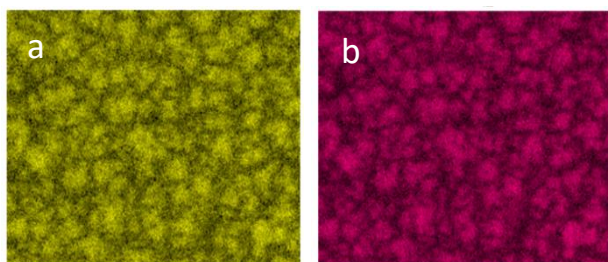


Figure 3. EDX mapping of AuPt deposited on ITO (a) Au (b) Pt.

The distribution of AuPt is homogeneously dispersed on the substrate, as shown in figure 3 of SEM-EDX mapping. The distribution of AuPt is homogeneously due to the presence of particles can influence growth and even particle size due to limiting particle nucleation, so particle growth is better due to the particles have reached thermodynamic stability and high electric current [31].

The decrease in DPPH absorbance is shown in Fig 4. AuPt nanoparticles can transfer electrons to DPPH-free radicals, thereby reducing DPPH to a stable non-radical compound [32]. The assumed scavenging mechanism is that gold nanoparticles will transfer their electrons and stabilize the N atoms contained in DPPH by bonding with each other [33]. The bond formed is a coordinating covalent bond. Therefore, DPPH becomes a non-radical compound with significant colour changes from purple to light pink in the incubation process for up to 210 minutes. The results of the DPPH test were then observed at a wavelength of 516 nm, and it is shown in Fig 5.

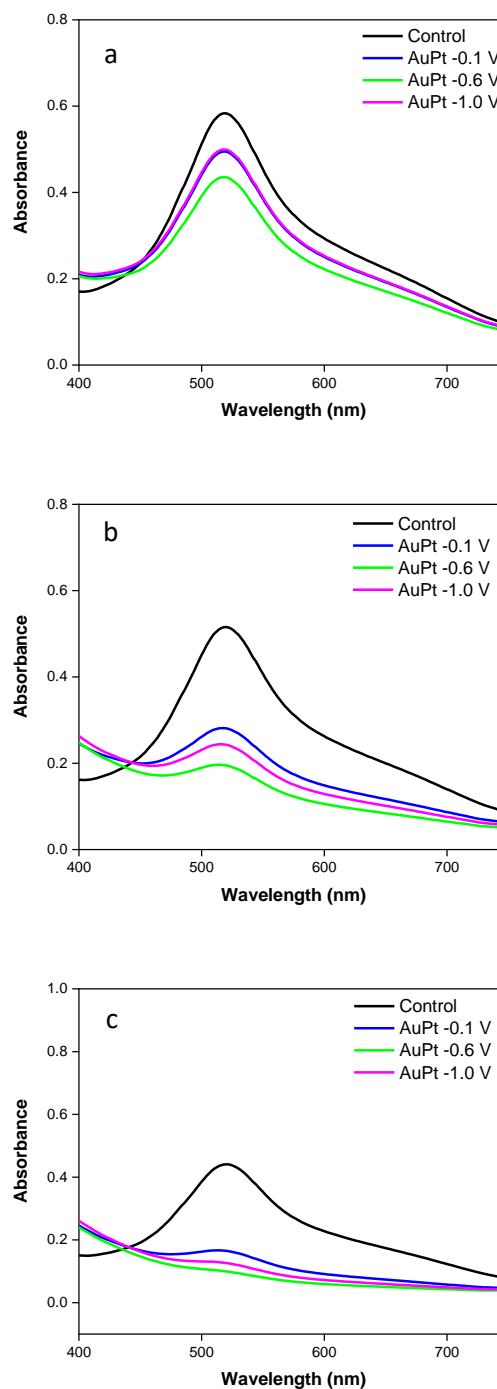


Figure 4. The absorbance curve for each sample of AuPt NPs in (a) 15 min, (b) 105 min, and (c) 210 min.

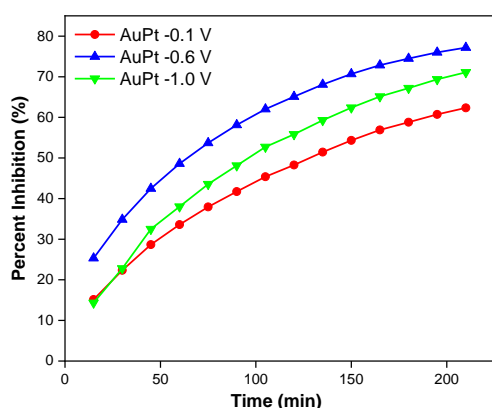


Figure 5. Inhibition percentage of AuPt NPs from 15 min to 210 min.

The results of this antioxidant activity test showed that the largest increase of inhibition percentage decrease in concentration was in AuPt NPs with an EL of -0.6 V. The result of the percent inhibition is 77.17%, which can be seen in Table 1. The highest inhibition percentage was achieved at AuPt NPs EI -0.6 V due to its size and the total amount of particles formed. The particle formed at -0.6 V is relatively smaller than at a lower potential of -1.0 V, and the number of particles is much greater than at a lower potential of -0.1 V, thus affecting the DPPH test results.

Table 1. Inhibition percentage of AuPt NPs.

Time (min)	Inhibition (%)		
	AuPt -0.1 V	AuPt -0.6 V	AuPt -1.0 V
15	15.15	25.33	14.34
30	22.34	34.84	22.79
45	28.66	42.48	32.50
60	33.60	48.61	38.03
75	37.96	53.71	43.55
90	41.72	58.14	48.20
105	45.40	62.02	52.73
120	48.27	65.10	55.82
135	51.44	68.08	59.28
150	54.33	70.68	62.40
165	56.90	72.85	65.12
180	58.81	74.48	67.19
195	60.73	76.01	69.37
210	62.34	77.17	71.09

4. Conclusion

AuPt nanoparticles have been successfully synthesized using the square-wave pulse deposition method. XRD results confirmed the formation of AuPt in each sample. Moreover, the morphology formed in the sample was irregular and spherical. The inhibition DPPH test results stated that AuPt at a lower potential (E_L) of -0.6 V had the highest antioxidant value, namely 77.17%, due to its relatively small size and large number of particles formed.

References

- [1] M. Khalil, E.S. Anggraeni, T.A. Ivandini, E. Budianto, Exposing TiO₂ (001) crystal facet in nano Au-TiO₂ heterostructures for enhanced photodegradation of methylene blue, *Appl. Surf. Sci.* **487** (2019) 1376–1384. <https://doi.org/10.1016/j.apsusc.2019.05.232>.
- [2] D. Benedec, I. Oniga, F. Cuibus, B. Sevastre, G. Stiuftuc, M. Duma, D. Hanganu, C. Iacovita, R. Stiuftuc, C.M. Lucaciu, Origanum vulgare mediated green synthesis of biocompatible gold nanoparticles simultaneously possessing plasmonic, antioxidant and antimicrobial properties, *Int. J. Nanomedicine*. **13** (2018) 1041–1058. <https://doi.org/10.2147/IJN.S149819>.
- [3] D. Wang, J. Markus, Y.J. Kim, C. Wang, Z.E. Jiménez Pérez, S.G. Ahn, V.C. Aceituno, R. Mathiyalagan, D.C. Yang, Coalescence of functional gold and monodisperse silver nanoparticles mediated by black Panax ginseng Meyer root extract, *Int. J. Nanomedicine*. **11** (2016) 6621–6634. <https://doi.org/10.2147/IJN.S113692>.
- [4] P.M. Anjana, M.R. Bindhu, M. Umadevi, R.B. Rakhi, Antibacterial and electrochemical activities of silver, gold, and palladium nanoparticles dispersed amorphous carbon composites, *Appl. Surf. Sci.* **479** (2019) 96–104. <https://doi.org/10.1016/j.apsusc.2019.02.057>.
- [5] D. Baruah, M. Goswami, R.N.S. Yadav, A. Yadav, A.M. Das, Biogenic synthesis of gold nanoparticles and their application in photocatalytic degradation of toxic dyes, *J. Photochem. Photobiol. B Biol.* **186** (2018) 51–58. <https://doi.org/10.1016/j.jphotobiol.2018.07.002>.
- [6] S.S. Godipurge, S. Yallappa, N.J. Biradar, J.S. Biradar, B.L. Dhananjaya, G. Hegde, K. Jagadish, G. Hegde, A facile and green strategy for the synthesis of Au, Ag and Au–Ag alloy nanoparticles using aerial parts of *R. hypocrateriformis* extract and their biological evaluation, *Enzyme Microb. Technol.* **95** (2016) 174–184. <https://doi.org/10.1016/j.enzmictec.2016.08.006>.
- [7] R.. Sekarsari, Taufikurrohmah, Sintesis dan Karakterisasi Nanogold dengan Variasi Konsentrasi HAuCl₄ sebagai Material Antiaging dalam Kosmetik,

- in: Pros. Semin. Nas. Kim. Unesa 2012- ISBN 978-979-028-550-7, 2012.
- [8] S. Pu, J. Li, L. Sun, L. Zhong, Q. Ma, An in vitro comparison of the antioxidant activities of chitosan and green synthesized gold nanoparticles, *Carbohydr. Polym.* **211** (2019) 161–172. <https://doi.org/10.1016/j.carbpol.2019.02.007>.
- [9] M.A. Amiruddin, T. Taufikurrohmah, SINTESIS DAN KARAKTERISASI NANOPARTIKEL EMAS MENGGUNAKAN MATRIKS BENTONIT SEBAGAI MATERIAL PEREDAM RADIKAL BEBAS DALAM KOSMETIK, *J. Chem.* **2** (2013) 68–75.
- [10] Q. Xiang, Y. Xu, R. Chen, C. Yang, X. Li, G. Li, D. Wu, X. Xie, W. Zhu, L. Wang, Electrodeposition of Pt₃Sn Nano-alloy on NiFe-Layered Double Hydroxide with “Card-house” Structure for Enhancing the Electrocatalytic Oxidation Performance of Ethanol, *ChemNanoMat.* **7** (2021) 314–322. <https://doi.org/10.1002/cnma.202000665>.
- [11] H. Burhan, M. Yilmaz, K. Cellat, A. Zeytun, G. Yilmaz, F. Şen, Direct ethanol fuel cells (DEFCs), in: Direct Liq. Fuel Cells Fundam. Adv. Futur., Elsevier, 2020: pp. 95–113. <https://doi.org/10.1016/B978-0-12-818624-4.00004-2>.
- [12] K.I. Ozoemena, S. Momeni, Elucidating the Effect of Additives on the Growth and Stability of Cu₂O Surfaces via Shape Transformation of Pre-Grown Crystals, *J. Am. Chem. Soc.* **170** (2018) 10356–10357. <https://doi.org/10.1016/j.microc.2018.07.035>.
- [13] Y. Zhang, C. Lu, G. Zhao, Z. Wang, Facile synthesis of gold-platinum dendritic nanostructures with enhanced electrocatalytic performance for the methanol oxidation reaction, *RSC Adv.* **6** (2016) 51569–51574. <https://doi.org/10.1039/c6ra06370e>.
- [14] Y. Zhao, L. Fan, J. Ren, B. Hong, Electrodeposition of Pt-Ru and Pt-Ru-Ni nanoclusters on multi-walled carbon nanotubes for direct methanol fuel cell, *Int. J. Hydrogen Energy.* **39** (2014) 4544–4557. <https://doi.org/10.1016/j.ijhydene.2013.12.202>.
- [15] S. Intarakamhang, A. Schulte, Automated electrochemical free radical scavenger screening in dietary samples, *Anal. Chem.* **84** (2012) 6767–6774. <https://doi.org/10.1021/ac301292c>.
- [16] S. Torres-Arellano, O. Reyes-Vallejo, J. Pantoja Enriquez, J.L. Aleman-Ramirez, A.M. Huerta-Flores, J. Moreira, J. Muñoz, L. Vargas-Estrada, P.J. Sebastian, Biosynthesis of cuprous oxide using banana pulp waste extract as reducing agent, *Fuel.* **285** (2021). <https://doi.org/10.1016/j.fuel.2020.119152>.
- [17] I. Ojea-Jiménez, N.G. Bastús, V. Puntès, Influence of the sequence of the reagents addition in the citrate-mediated synthesis of gold nanoparticles, *J. Phys. Chem. C.* **115** (2011) 15752–15757. <https://doi.org/10.1021/jp2017242>.
- [18] C. Daruich De Souza, B. Ribeiro Nogueira, M.E.C.M. Rostelato, Review of the methodologies used in the synthesis gold nanoparticles by chemical reduction, *J. Alloys Compd.* **798** (2019) 714–740. <https://doi.org/10.1016/j.jallcom.2019.05.153>.
- [19] I.A. Mohammed, F.J. Al-Gawhari, Gold nanoparticle: Synthesis, functionalization, enhancement, drug delivery and therapy: A review, *Syst. Rev. Pharm.* **11** (2020) 888–910. <https://doi.org/10.31838/srp.2020.6.127>.
- [20] K. Shi, M. Ren, I. Zhitomirsky, Activated Carbon-Coated Carbon Nanotubes for Energy Storage in Supercapacitors and Capacitive Water Puri fication, (2014).
- [21] I. Gurrappa, L. Binder, Electrodeposition of Nanostructured Coatings and their Characterization - A Review, *Sci. Technol. Adv. Mater.* **9** (2008). <https://doi.org/10.1088/1468-6996/9/4/043001>.
- [22] H. Syafei, Dwi Giwang Kurniawan, Electrodeposition of Co_xNi_y Thin Film and Its Catalytic Activity for Ethanol Electrooxidation, *Chem. Mater.* **2** (2023) 14–18. <https://doi.org/10.56425/cma.v2i1.50>.
- [23] S. Budi, R.A. Tawwabin, U. Cahyana, Afriza, M. Paristiwati, Saccharin-assisted galvanostatic electrodeposition of nanocrystalline FeCo films on a flexible substrate, *Int. J. Electrochem. Sci.* **15** (2020) 6682–6694. <https://doi.org/10.20964/2020.07.74>.
- [24] B.A. Suliasih, A. Sakinah, M. Angelina, The Effect of Electrodeposition Voltage on the Antioxidant Activity of Gold Nanoparticles, **3** (2024) 27–33.
- [25] T.-H. Lin, W.-H. Hung, Electrochemical Deposition of Gold Nanoparticles on a Glassy Carbon Electrode Modified with Sulfanilic Acid, *J. Electrochem. Soc.* (2009). <https://doi.org/10.1149/1.3033524>.
- [26] F. Xiao, F. Zhao, Y. Zhang, G. Guo, B. Zeng, Ultrasonic electrodeposition of gold - platinum alloy nanoparticles on ionic liquid - chitosan composite film and their application in fabricating nonenzyme hydrogen peroxide sensors, *J. Phys. Chem. C.* **113** (2009) 849–855. <https://doi.org/10.1021/jp808162g>.
- [27] Q. Yu, L. Qian, W. Qiu, Y. Miao, J. Zhang, Y. Wang, AuPt nanoalloy with dual functionalities for sensitive detection of HPV16 DNA, *RSC Adv.* **13** (2023) 13940–13946. <https://doi.org/10.1039/d3ra00757j>.
- [28] A.J. Wang, K.J. Ju, Q.L. Zhang, P. Song, J. Wei, J.J. Feng, Folic acid bio-inspired route for facile synthesis of AuPt nanodendrites as enhanced electrocatalysts for methanol and ethanol oxidation reactions, *J. Power Sources.* **326** (2016) 227–234. <https://doi.org/10.1016/j.jpowsour.2016.06.115>.
- [29] H.C. Chiang, Y. Wang, Q. Zhang, K. Levon, Optimization of the electrodeposition of gold nanoparticles for the application of highly sensitive, label-free biosensor, *Biosensors.* **9** (2019). <https://doi.org/10.3390/bios9020050>.
- [30] N. Naderi, M.R. Hashim, J. Rouhi, N. Naderi, J. Rouhi, Synthesis and Characterization of Pt Nanowires Electrodeposited into the Cylindrical Pores of

- Polycarbonate Membranes, 2012. www.electrochemsci.org.
- [31] H.B. Hassan, Z.A. Hamid, R.M. El-Sherif, Electrooxidation of methanol and ethanol on carbon electrodeposited Ni-MgO nanocomposite, *Cuihua Xuebao/Chinese J. Catal.* **37** (2016) 616–627. [https://doi.org/10.1016/S1872-2067\(15\)61034-8](https://doi.org/10.1016/S1872-2067(15)61034-8).
- [32] R.A. Zayadi, F.A. Bakar, Comparative study on stability, antioxidant and catalytic activities of bio-stabilized colloidal gold nanoparticles using microalgae and cyanobacteria, *J. Environ. Chem. Eng.* **8** (2020). <https://doi.org/10.1016/j.jece.2020.103843>.
- [33] S. Priya Velammal, T.A. Devi, T.P. Amaladhas, Antioxidant, antimicrobial and cytotoxic activities of silver and gold nanoparticles synthesized using *Plumbago zeylanica* bark, *J. Nanostructure Chem.* **6** (2016) 247–260. <https://doi.org/10.1007/s40097-016-0198-x>.